

Paired Dislocations and Their Interactions with γ' Particles in Polycrystalline Superalloy GH4037

Xianzi Lv, Fei Sun, Jinyan Tong, Qiang Feng, and Jianxin Zhang

(Submitted May 3, 2014; in revised form August 10, 2014; published online November 15, 2014)

The microstructural characteristics of nickel-based polycrystalline superalloy GH4037 turbine blades that have been in service for 1600 h have been studied by transmission electron microscopy. In particular, emphasis has been placed on paired dislocations and their interactions with γ' precipitates. Paired dislocations are universal and coexist with Orowan loops occasionally. The attractive force due to anti-phase boundary energy and the repulsive force between two $1/2 \langle 110 \rangle$ dislocations act on paired dislocations simultaneously, causing different morphologies of edge dislocations. Since the shear stress required by paired dislocations to cut through γ/γ' structure is much lower than Orowan stress of single matrix dislocation, the major formation mechanism is dislocation pairing. A large number of paired dislocations slipping on the same $\{111\}$ plane can form slip band and can shear off γ' particles, which may directly lead to the formation of microcracks.

Keywords Orowan loop, paired dislocations, slip band, γ' particle

1. Introduction

Gas turbine engines are widely used in the fields of aircraft and some military equipment (Ref 1, 2). Their lifetime correlates strongly with the performance of internal turbine blades, since turbine blades must withstand complicated load under static, fatigue, and creep conditions (Ref 2-4). The function of turbine blades is to convert work coming from gas stream into mechanical energy, which can drive the high-pressure compressor (Ref 2). Superalloys have an ability to resist extreme load over extended periods of time, becoming unique high-temperature materials used in turbine blades. In order to prolong the service life of turbine blades, considerations should be given to the failure modes, together with their strong dependence on microstructures and defects.

For turbine blades, there exist normal failure modes and abnormal failure modes. Normal failure modes refer to not only visible damages including abrasive wear, internal cracking, and

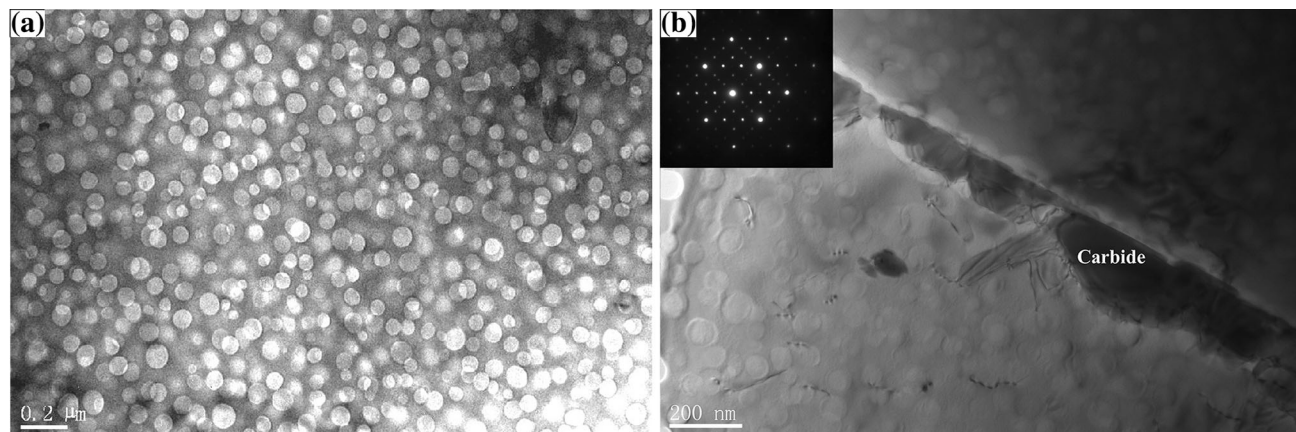
segmental falling, but also internal damages of metallographic structures (Ref 5-7). Microstructural damages can occur when temperature and stress are below the critical values, covering coarsening of γ' precipitates, morphological changes of γ/γ' interfaces and carbides, and formation of brittle phases. γ matrix, γ' precipitate, carbides, and borides are the typical microstructural phases of a superalloy (Ref 2). Some important forms of normal failure consist of creep, low-cycle fatigue, thermal fatigue, and mixed interactions among them (Ref 5). In addition, abnormal failures are caused by nonstandard operation, defects introduced during preparative process, and improper designs. Some representative abnormal failure modes include high-cycle fatigue and over-heating induced by higher temperature.

The nickel-based polycrystalline superalloy GH4037 was prepared using an aging process. The aging process refers to the heat treatment where the part is a period of time at a constant temperature to precipitate out all γ' phases. More W and Mo were added for solution strengthening, and B can strengthen grain boundaries (Ref 8, 9). GH4037 possesses structural stability and excellent compressive properties during 800-850°C, and has been widely used for turbine blades of aircraft engines. It turns out that the mechanical properties displayed by superalloys are strongly dependent upon dislocations and their interactions with γ' particles (Ref 2). There exist two models for paired dislocations in the $\langle 110 \rangle$ direction on the $\{111\}$ plane to pass through γ' precipitates. The first model represents “weakly” paired dislocations to cut through ordered particles (Ref 10, 11). The second one represents “strongly” coupled dislocations to cut through larger particles (Ref 11, 12). It has also been reported that Orowan loops were rarely found in turbine disk materials (Ref 13). In this paper, attention is focused on the microstructural characteristics of turbine blade which has been in service for 1600 h. Great emphasis is placed on the reason why formation of paired dislocations is the main mechanism and their influences on properties of superalloy. This provides an excellent chance to know more about the nature of performance degradation of turbine blades.

Xianzi Lv and **Fei Sun**, Key Laboratory of Liquid Structure and Heredity of Materials, Ministry of Education, Shandong University, 17923 Jingshi Road, Jinan 250061 Shandong Province, China; **Jinyan Tong**, National Center for Materials Service Safety, University of Science and Technology Beijing, Beijing 100083, China; **Qiang Feng**, National Center for Materials Service Safety, University of Science and Technology Beijing, Beijing 100083, China and State Key Laboratory for Advanced Metals and Materials, University of Science and Technology Beijing, Beijing 100083, China; **Jianxin Zhang**, Key Laboratory of Liquid Structure and Heredity of Materials, Ministry of Education, Shandong University, 17923 Jingshi Road, Jinan 250061 Shandong and School of Materials Science and Engineering, Shandong University, 17923 Jingshi Road, Jinan, Shandong Province 250061, China. Contact e-mail: jianxin@sdu.edu.cn.

Table 1 Nominal compositions of GH4037 superalloy in wt.%

	C	Cr	W	Mo	Al	Ti	V	Fe
Wt.%	0.03-0.10	13.0-16.0	5.0-7.0	2.0-4.0	1.7-2.3	1.8-2.3	0.1-0.5	5.0
	B	Mn	Si	P	S	Ce	Ni	
Wt.%	0.02	0.5	0.4	0.015	0.01	0.07	Bal	

**Fig. 1** Typical microstructures of superalloy GH4037

2. Experimental

The nominal composition of nickel-based polycrystalline superalloy GH4037, in weight percent, is shown in Table 1. It is worth noting that the contents of C and Si should be strictly controlled because they show strong correlations with the permanence properties and impact toughness of superalloy GH4037 (Ref 8). According to the China Aeronautical Materials Handbook, GH4037 was solution heat treated at 800°C for 16 h after a two-stage aging process with heating to 1180°C for 2 h and 1050°C for 4 h (Ref 9). After the first stage, most γ' precipitates are dissolved in γ matrix. Then some particles are precipitated out after the second stage. The typical microstructure of GH4037 after heat treatment consists of γ matrix and dispersed γ' precipitates as shown in Fig. 1a. Few carbides are distributed around grain boundaries, and block MC-type carbides can be found within grain interiors. The γ' precipitates are spherical, with an average size being 100 nm. The γ' phase is made of $(\text{Ni}_{0.97}\text{Cr}_{0.02}\text{V}_{0.01})_{3.05}(\text{Al}_{0.56}\text{Ti}_{0.27}\text{W}_{0.03}\text{Cr}_{0.08}\text{Mo}_{0.02})$, and its lattice parameter is about 0.3572-0.3575 (Ref 8). The volume fraction of γ' particles is about 20% and will be larger if kept at 800°C for 500-1500 h during the aging process.

The blade selected for this study has been in service for 1600 h without repair, replacement, and heat treatment. Microstructures were examined using Tecnai T20 transmission electron microscope (TEM) and JEOL 2010F instruments (Beijing University of Technology, China) under an acceleration voltage of 200 kV and a point resolution of 0.19 nm. To prepare TEM samples, slices were cut from two-thirds site of the airfoil, and were mechanically punched into 3 mm in diameter and thinned to about 30 μm in thickness. Then, they were further electrochemical polished with a double jet polisher using a solution of 20% perchloric acid in ethanol at -20°C .

3. Results and Discussion

From TEM observations, γ' particles in superalloy GH4037 are spherical, and dispersedly distributed in the continuous γ matrix phase, as shown in Fig. 1(a). The sizes of γ' particles mainly vary from 50 to 120 nm, and some carbides can be found (see Fig. 1b), as the case for the over-aged condition. Among them, the presence of paired dislocations is representative.

4. Morphological Characteristics of Paired Dislocations

Figure 2 shows clearly that paired dislocations traveled through γ/γ' structure in GH4037 with different morphologies. It has been reported that cutting of γ' particle by paired dislocations can lead to the formation of antiphase boundary (APB) between them within γ' phase (Ref 14-16). The first $1/2 <110>$ dislocation produces the APB, and the second one removes it. Thus, they exist in pairs in general. In Fig. 2(a), the leading dislocation (marked as D_1) bowed out between γ' particles strongly and interacted with spheres, while the trailing dislocation (marked as D_2) did not enter γ' precipitates or was pinned in the γ/γ' interface. D_2 can be treated as a straight line because it nearly followed the whole curvature of D_1 . In Fig. 2(b), D_1 and D_2 of paired dislocations all cut through γ' precipitates in varying degrees. One should note that the spacing of paired dislocations, a few tens of nanometers, is comparable to the particle diameter.

It should be recognized from above observations that the relative positions of paired dislocations and γ' particles may vary to some extent, as shown in Fig. 3(a). The appearance of coupled dislocations varies largely. These different morphologies

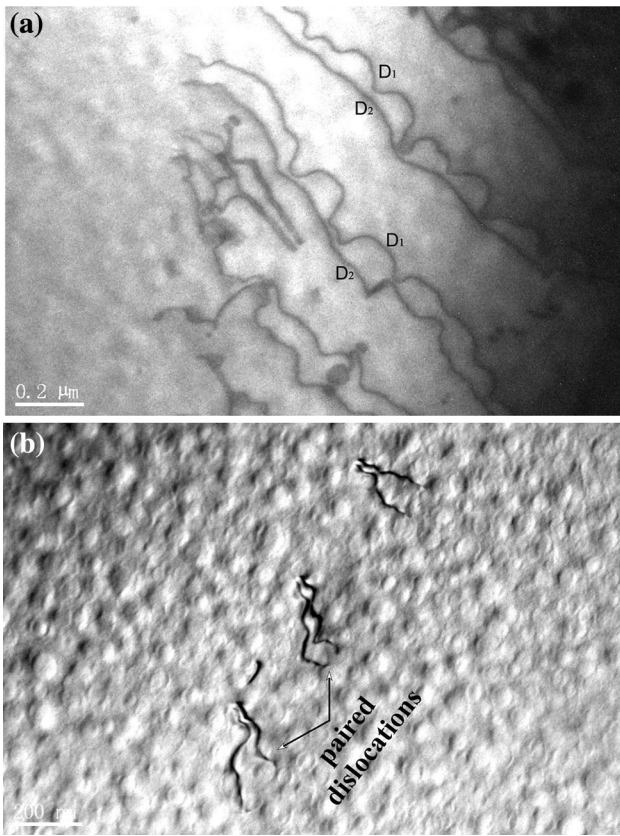


Fig. 2 Paired dislocations interact with γ' particles in superalloy GH4037

of paired dislocations can be rationalized as follows: the formation of dislocation pairing is determined by the following factors (Ref 17): (I) the force introduced by applied shear stress, equals to $\tau b d_i$ ($i = 1, 2$), in which τ stands for the shear stress required by a $1/2 \langle 110 \rangle$ dislocation to travel through the γ/γ' structure, and d is the distance between two neighboring particles along the leading or trailing dislocation, as demonstrated in Fig. 3(a); b stands for the magnitude of the Burgers vector of the $1/2 \langle 110 \rangle$ dislocation. (II) The attractive force due to the APB energy is equivalent to $\gamma_{APB} l_i$ ($i = 1, 2$), in which l stands for line length of paired dislocations inside particles, and γ_{APB} represents the APB energy on $\{111\}$ planes; (III) the repulsive force (or elastic force) as a consequence of dislocations with the same sense, marked as σ . Therefore, the balance of total stresses for D_1 and D_2 will be expressed, respectively, as follows (Ref 2).

$$\text{For } D_1 \quad \tau b d_1 + \sigma - \gamma_{APB} l_1 = 0, \quad (\text{Eq 1})$$

$$\text{For } D_2 \quad \tau b d_2 - \sigma + \gamma_{APB} l_2 = 0. \quad (\text{Eq 2})$$

Since the leading dislocation (D_1) tries to introduce an APB and the trailing dislocation (D_2) is trying to remove it, the attractive forces have opposite signs in the above equations. The attractive force due to APB energy can push D_2 to slip forward, causing small separation between D_1 and D_2 ; however, the repulsive force will compel D_2 to slip backward, leading to larger separation. They are influenced by the values of d and r (the radius of γ' particle, as shown in Fig. 3b)

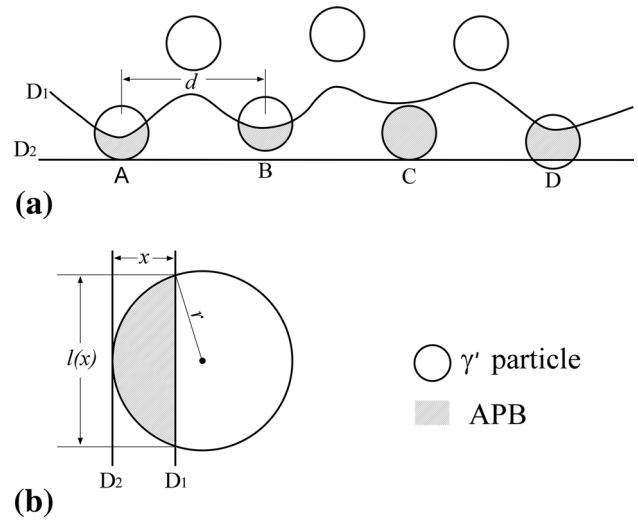


Fig. 3 (a) Different morphologies of paired dislocations; (b) when $l_1 - l_2$ reaches a minimum, the relative position of paired dislocations and γ' particle

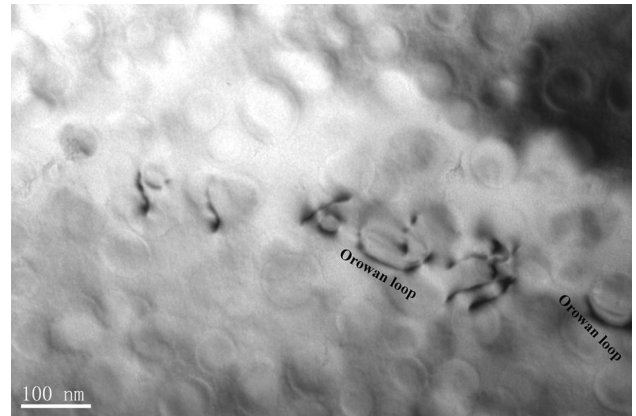


Fig. 4 Orowan loops encircle γ' particles in GH4037

significantly, so the width of APB (the separation distance of paired dislocations) changes distinctly.

5. Coexistence with Orowan Loops

Orowan loops encircled γ' particles can be observed in the specimens, as shown in Fig. 4. Dislocations were confined within the γ matrix and could not shear γ' phases. When the matrix dislocations attempted to by-pass the γ' particles, irregular loops around precipitates were left behind. Orowan loops are supposed to form in the process of dislocation by-passing.

Figure 5 describes the coexistence of paired dislocations and Orowan loops. At high stress and high temperature (870°C and 300 MPa), dislocation by-passing process occurred, and Orowan loops can be found for superalloy GTD-111 (Ref 18). For superalloy IN 713C, Orowan loops existed in the specimens aged 2 h at 1000°C (Ref 19). Jackson and Reed have observed coupled dislocations in U720Li samples aged at 700°C for 60 h (Ref 11).

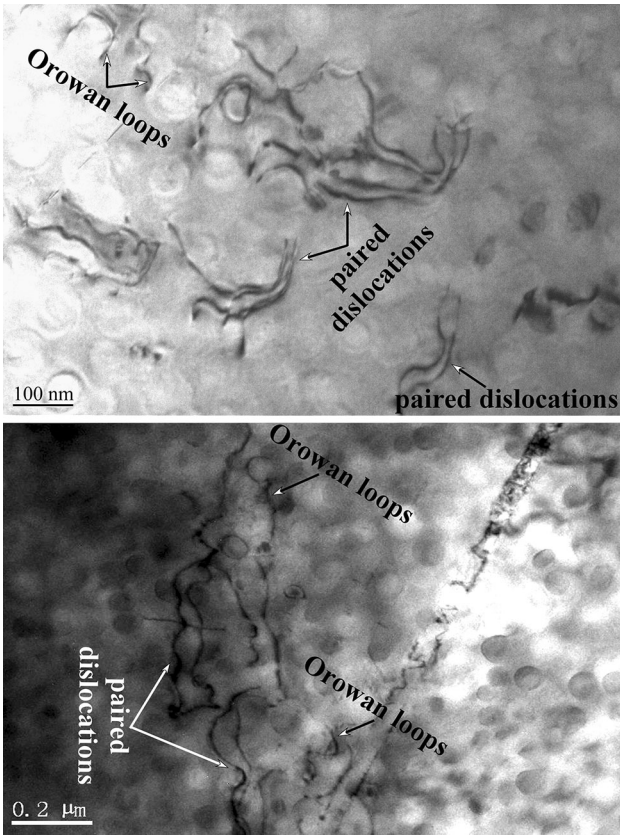


Fig. 5 Paired dislocations (which are in quantity) coexist with Orowan loops in GH4037

Based on Fig. 4 and 5, the amount of paired dislocations is much larger than that of Orowan loops. The practical temperature field and stress field where the chosen turbine blade worked would change continuously over operating time. If the temperature and the stress are all helpful for dislocation by-passing process and dislocation pairing, they can occur arbitrarily. However, the reason why the process of dislocation by-passing is a rare occurrence will be analyzed in the following section.

6. The Major Formation Mechanism in GH4037 is Dislocation Pairing

As before, it should be recognized that the major formation mechanism in GH4037 is dislocation coupling, other than Orowan mechanism. Attention should be focused on the critical resolved shear stress (CRSS) required by paired dislocations to cut through γ' particles.

The trailing dislocation must overcome the elastic force (repulsive force) to enter γ' particles, and consequently, its behaviors depend strongly on the repulsive force σ . In this study, assume d_1 and d_2 to be equal in magnitude and be approximated by d for the sake of simplified calculation. Then after some manipulations, one can obtain

$$(1) + (2)2\tau bd + \gamma_{\text{APB}}(l_2 - l_1) = 0, \quad (\text{Eq 3})$$

$$(1) - (2)2\sigma = \gamma_{\text{APB}}(l_1 + l_2). \quad (\text{Eq 4})$$

so that

$$\tau = \frac{1}{2bd}\gamma_{\text{APB}}(l_1 - l_2). \quad (\text{Eq 5})$$

This implies that τ depends critically upon the difference values of the line length l_1, l_2 . Provided that the line length $l(x)$ is a function of x , $l(x)$ can be expressed as $l(x) = 2[r^2 - (r - x)^2]^{1/2}$ according to the geometric relationship shown in Fig. 3(b). When the trailing dislocation (D_2) just touches the γ' particle, the difference in the values $l_1 - l_2$ will reach a minimum. At this point, $l_2 = 0$ and $l_1 = l(x_1)$ if the position of the leading dislocation (D_1) is defined as x_1 . Then Eqs 3 and 4 can be written as

$$2\tau bd = \gamma_{\text{APB}}l(x_1) = 2\sigma. \quad (\text{Eq 6})$$

That is to say, the value of τ shows a dependence on σ directly. While the magnitude of σ can be estimated to be $Gb^2/(2\pi x)$ on the basis of dislocation theory (Ref 20), where G stands for the elastic shear modulus. Taking small uncertainties into account and introducing a dimensionless constant α , σ is given by

$$\sigma = \frac{Gb^2\alpha l(x_1)}{2\pi x_1}. \quad (\text{Eq 7})$$

Consequently, the force τ can be shown to be

$$\tau = \frac{Gb\alpha l(x_1)}{2\pi d x_1}. \quad (\text{Eq 8})$$

Thus, the CRSS required by paired dislocations to cut through γ' particles can be obtained:

$$\tau_c = \frac{Gb}{2\pi d}(2\alpha)\left(\frac{2r}{x_1} - 1\right)^{1/2}, \quad (\text{Eq 9})$$

where

$$x_1 = \frac{Gb^2 2\alpha}{2\pi \gamma_{\text{APB}}}. \quad (\text{Eq 10})$$

By substituting Eq 10 into Eq 9, one can obtain

$$\tau_c = \frac{Gb}{2\pi d}(2\alpha)\left(\frac{2r\pi\gamma_{\text{APB}}}{\alpha Gb^2} - 1\right)^{1/2}. \quad (\text{Eq 11})$$

To obtain the critical condition, the following parameters are adopted: $r = 100$ nm, $G = 80$ GPa (Ref 11), $\gamma_{\text{APB}} = 0.1$ J/m² (Ref 2), $b = (\sqrt{2}/2)a$, $a = 0.253$ nm, and $\alpha = 1$. [α is of the order of unity, which accounts for the elastic repulsion between the strongly paired dislocations (Ref 11)]. The Orowan stress τ_{Orowan} is defined as Gb/d , so that the relationship between τ_c and τ_{Orowan} is given as

$$\tau_c = 0.47 \frac{Gb}{d} = 0.47\tau_{\text{Orowan}}. \quad (\text{Eq 12})$$

Equation 11 suggests that the CRSS for dislocation pairing is 53% lower than the Orowan bowing stress, so it is more difficult for single matrix dislocation to by-pass γ' particle. Inversely, paired dislocations can cut through γ' phase more easily; therefore, there exist more paired dislocations than Orowan loops in the specimens. This equation not only offers a qualitative relationship between the CRSS of paired dislocations and the Orowan stress, but also provides direct proof for experimental observations. The major strengthening mechanism is dislocation pairing rather than the Orowan mechanism.

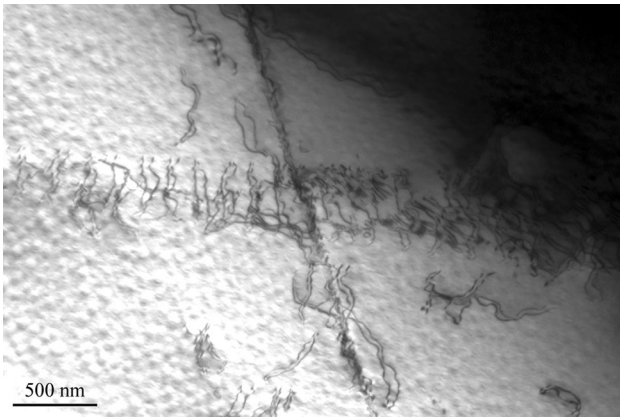


Fig. 6 Slip band composed of paired dislocations cut through γ/γ' structure in GH4037

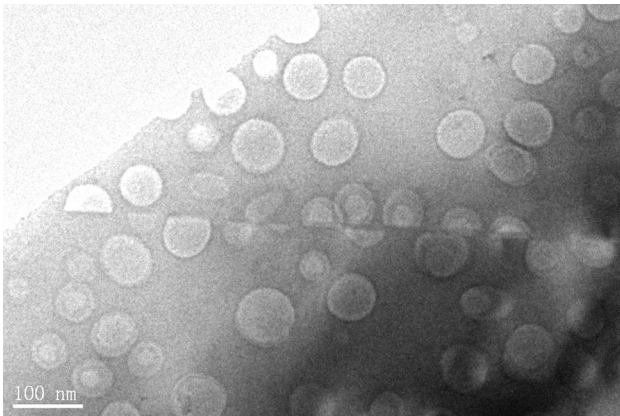


Fig. 7 Shearing of γ' particles by paired dislocations in GH4037

7. Slip Band Composed of Paired Dislocations

Figure 6 shows details of a representative slip band, width of which is about 500 nm. Note that the slip band consists of high density of paired dislocations, cutting through both γ' precipitates and γ matrix. The slip band initiated from the site of stress concentration, which can be inferred from intense contrast. Cutting of γ' particles by paired dislocations brought a positive APB energy within γ' particles. This also promotes planar deformation and leads to softening on active slip planes by means of making cross-slip difficult (Ref 21). Deformation in this case was planar and inhomogeneous, introducing some intense slip bands.

Figure 7 describes shearing of γ' particles in GH4037. When a $1/2 \langle 110 \rangle$ dislocation swept over $\{111\}$ slip plane, slip proceeded a Burger vector \mathbf{b} in the ordered crystal, and the magnitude of \mathbf{b} was equal to an atomic separation of 0.2 nm. Roughly, the segments of γ' particles that appear to be sheared off in Fig. 7 were attributed to 200 dislocation pairs.

It has been reported that the crack was found to occur along the slip band (Ref 13, 22, 23). The failure mode of turbine blade can be assumed as follows—combined TEM results with those of previous papers. There exist stress concentrations around some intrinsic defects, offering good opportunity for paired dislocations to bow out and slip along certain $\{111\}$ plane. When local stress accumulates, a great number of paired

dislocations emerge and slip successively, forming a slip band. A microcrack can occur following the slip band, and propagation and increment of cracks lead to the failure of superalloy GH4037 finally.

For GH4037 superalloy, a matrix dislocation cannot cut into γ' particles without the formation of APB, and thus, dislocations must travel through γ/γ' structure in pairs. Strengthening by γ' particles in this paper is influenced by shear modulus, APB energy, interfacial energy, and Orowan strengthening. If the applied stress is higher than the critical shear stress, slip band will form with the increasing dislocations, which can lead to the formation of microcracks. Hence, keeping the GH4037 superalloy under the critical working condition can prolong the service life of turbine blade.

8. Conclusions

The microstructural evolution of superalloy GH4037 cut from serviced turbine blade has been observed in detail, and some analyses focused on paired dislocations have been made to study the microstructural formation mechanism of superalloy. Several conclusions can be drawn from the following list.

- (1) The attractive force due to the APB energy and the repulsive force between dislocations with the same sense determine the width of APB and the morphology of dislocation lines.
- (2) Dislocation pairing and dislocation by-passing process can occur arbitrarily under complicated service condition, but the amount of dislocation pairs is much larger than that of Orowan loops.
- (3) The CRSS required for dislocation pairing is about 53% lower than the Orowan stress, so the major formation mechanism during the service of GH4037 is one of dislocation pairing.
- (4) The continuous occurrence and slip of paired dislocations along the same slip plane cause the shear-off of γ' precipitates and the formation of slip band. Microcracks may happen along slip band and lead to the failure of superalloy.

Acknowledgments

This work was supported by the National Natural Science Foundation of China (Grant No. 50971078, No. 51071096, No. 51271097, and No. 50671015), Shandong Province Natural Science Foundation (Grant No. ZR2010EM009), China Postdoctoral Science Foundation (special grade, Grant No. 201003630), and the National Basic Research Program of China (No. 2010CB631201).

References

1. T.M. Pollock and S. Tin, Nickel-Based Superalloys for Advanced Turbine Engines: Chemistry, Microstructure and Properties, *J. Propuls. Power*, 2006, **22**(2), p 361–374
2. R.C. Reed, *The Superalloys Fundamentals and Applications*, 1st ed., Cambridge University Press, New York, 2006
3. J. Lankford and S.J. Hudak, Jr., Relevance of the Small Crack Problem to Lifetime Prediction in Gas Turbines, *Int. J. Fatigue*, 1987, **9**(2), p 87–93

4. Z. Mazur, A. Luna-Ramirez, J.A. Juarez-Islas, and A. Campos-Amezcuca, Failure Analysis of a Gas Turbine Blade Made of Inconel 738LC Alloy, *Eng. Fail. Anal.*, 2005, **12**(3), p 474–486
5. T.J. Carter, Common Failures in Gas Turbine Blades, *Eng. Fail. Anal.*, 2005, **12**(2), p 237–247
6. E. Poursaeidi, M. Aieneravaie, and M.R. Mohammadi, Failure Analysis of a Second Stage Blade in a Gas Turbine Engine, *Eng. Fail. Anal.*, 2008, **15**(8), p 1111–1129
7. C.J. McMahon, Jr., On the Mechanism of Premature In-Service Failure Nickel-Base Superalloy Gas Turbine Blades, *Mater. Sci. Eng.*, 1974, **13**(3), p 295–297
8. J.T. Guo, *Materials Science and Engineering for Superalloys*, 1st ed., Science Press, Beijing, 2008 (in Chinese)
9. Editorial Committee of China Aeronautical Materials Handbook, *China Aeronautical Materials Handbook*, 2nd ed., China Standards, Beijing, 2002 (in Chinese)
10. L.M. Brown and R.K. Ham, *Strengthening Mechanisms in Crystals*, 1st ed., Applied Science, London, 1971
11. M.P. Jackson and R.C. Reed, Heat Treatment of UDIMET 720Li: The Effect of Microstructure on Properties, *Mater. Sci. Eng.*, 1999, **A259**(1), p 85–97
12. W. Huther and B. Reppich, Interaction of Dislocation with Coherent, Stress-Free, Ordered Precipitates, *Z. Metall.*, 1978, **69**(19), p 628–634
13. A. Shyam and W.W. Milligan, A Model for Slip Irreversibility, and Its Effect on the Crack Propagation Threshold in a Nickel-Base Superalloy, *Acta Mater.*, 2005, **53**(3), p 835–844
14. E. Nembach, K. Suzuki, M. Ichihara, and S. Takeuchi, In-Situ Deformation of the Gamma Prime Hardened Superalloy Nimonic PE16 in High-Voltage Electron Microscopes, *Philos. Mag.*, 1985, **A51**(4), p 607–618
15. B. Reppich, Some New Aspects Concerning Particle Hardening Mechanisms in γ' Precipitating Ni-Base Alloys—I. Theoretical Concept, *Acta Metall.*, 1982, **30**(1), p 87–94
16. B. Reppich, P. Schepp, and G. Wehner, Some New Aspects Concerning Particle Hardening Mechanisms in γ' Precipitating Ni-Base Alloys—II. Experiments, *Acta Metall.*, 1982, **30**(1), p 95–104
17. F. Sun, S. Zhang, S.G. Tian, J.X. Zhang, and H. Harada, Large Stress Concentrations Around Micropore Near a Crack-Tip Induced Deformation Twinning in Ni-Based Single Crystal Superalloy, *J. Alloy. Compd.*, 2014, **586**(15), p 479–484
18. S. Nategh and S.A. Sajjadi, Dislocation Network Formation During Creep in Ni-Base Superalloy GTD-111, *Mater. Sci. Eng.*, 2003, **A339**(1-2), p 103–108
19. A.K. Singh, N. Louat, and K. Sadananda, Dislocation Network Formation and Coherency Loss Around Gamma-Prime Precipitates in a Nickel-Base Superalloy, *Metall. Trans.*, 1988, **A19**(12), p 2965–2973
20. J.P. Hirth and J. Lothe, *Theory of Dislocations*, 2nd ed., Wiley, New York, 1982
21. J.E. King, Fatigue Crack Propagation in Nickel-Base Superalloys—Effects of Microstructures, Load Ratio, and Temperature, *Mater. Sci. Technol.*, 1987, **3**(9), p 750–763
22. K.S. Chin, J.E. Hack, and G.R. Leverant, Fatigue Crack Propagation in Ni-Base Superalloy Single Crystals Under Multiaxial Cyclic Loads, *Metall. Trans.*, 1986, **A17**(10), p 1739–1750
23. M. Petre nec, K. Obrtlík, and J. Polak, Inhomogeneous Dislocation Structure in Fatigued INCONEL 713LC Superalloy at Room and Elevated Temperatures, *Mater. Sci. Eng.*, 2005, **A400-401**(25), p 485–488